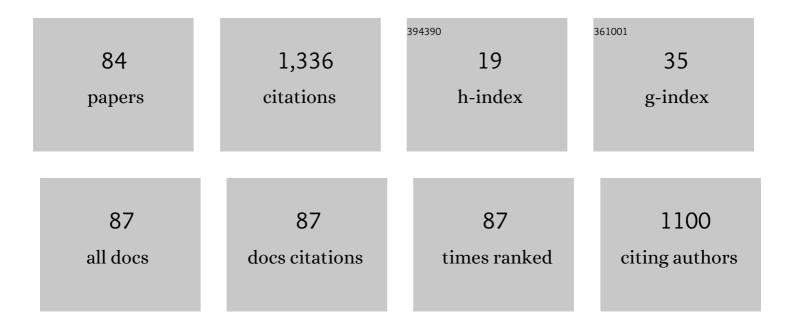
Seungwon Lee

List of Publications by Year in descending order

Source: https://exaly.com/author-pdf/7345346/publications.pdf Version: 2024-02-01



#	Article	IF	CITATIONS
1	Influence of dislocation–solute atom interactions and stacking fault energy on grain size of single-phase alloys after severe plastic deformation using high-pressure torsion. Acta Materialia, 2014, 69, 68-77.	7.9	173
2	Precipitation kinetics in a severely plastically deformed 7075 aluminium alloy. Acta Materialia, 2014, 66, 105-117.	7.9	111
3	Formation of FeNi with <i>L</i> 1 ₀ -ordered structure using high-pressure torsion. Philosophical Magazine Letters, 2014, 94, 639-646.	1.2	79
4	High-pressure torsion of titanium at cryogenic and room temperatures: Grain size effect on allotropic phase transformations. Acta Materialia, 2014, 68, 207-213.	7.9	78
5	Age hardening and thermal stability of Al–Cu alloy processed by high-pressure torsion. Materials Science & Engineering A: Structural Materials: Properties, Microstructure and Processing, 2015, 627, 111-118.	5.6	70
6	Atomic scale HAADF-STEM study of η′ and η 1 phases in peak-aged Al–Zn–Mg alloys. Journal of Materials Science, 2018, 53, 4598-4611.	3.7	62
7	Microstructures and Mechanical Properties of Pure V and Mo Processed by High-Pressure Torsion. Materials Transactions, 2010, 51, 1072-1079.	1.2	55
8	Strengthening of Cu–Ni–Si alloy using high-pressure torsion and aging. Materials Characterization, 2014, 90, 62-70.	4.4	50
9	Age-hardening of an Al–Li–Cu–Mg alloy (2091) processed by high-pressure torsion. Materials Science & Engineering A: Structural Materials: Properties, Microstructure and Processing, 2012, 546, 82-89.	5.6	48
10	High-Pressure Torsion for Pure Chromium and Niobium. Materials Transactions, 2012, 53, 38-45.	1.2	45
11	Concurrent strengthening of ultrafine-grained age-hardenable Al-Mg alloy by means of high-pressure torsion and spinodal decomposition. Acta Materialia, 2017, 131, 57-64.	7.9	45
12	Strengthening of A2024 alloy by high-pressure torsion and subsequent aging. Materials Science & Engineering A: Structural Materials: Properties, Microstructure and Processing, 2017, 704, 112-118.	5.6	45
13	Continuous high-pressure torsion using wires. Journal of Materials Science, 2012, 47, 473-478.	3.7	44
14	Methods for Designing Concurrently Strengthened Severely Deformed Age-Hardenable Aluminum Alloys by Ultrafine-Grained and Precipitation Hardenings. Metallurgical and Materials Transactions A: Physical Metallurgy and Materials Science, 2013, 44, 3921-3933.	2.2	43
15	Strengthening of AA7075 alloy by processing with high-pressure sliding (HPS) and subsequent aging. Materials Science & Engineering A: Structural Materials: Properties, Microstructure and Processing, 2015, 628, 56-61.	5.6	38
16	High strength and superconductivity in nanostructured niobium–titanium alloy by high-pressure torsion and annealing: Significance of elemental decomposition and supersaturation. Acta Materialia, 2014, 80, 149-158.	7.9	33
17	Aging Behavior of Al 6061 Alloy Processed by High-Pressure Torsion and Subsequent Aging. Metallurgical and Materials Transactions A: Physical Metallurgy and Materials Science, 2015, 46, 2664-2673.	2.2	31
18	Superconducting properties in bulk nanostructured niobium prepared by high-pressure torsion. Physica C: Superconductivity and Its Applications, 2013, 493, 132-135.	1.2	25

#	Article	IF	CITATIONS
19	Extra Electron Diffraction Spots Caused by Fine Precipitates Formed at the Early Stage of Aging in Al-Mg-X (X=Si, Ge, Zn)-Cu Alloys. Materials Transactions, 2017, 58, 167-175.	1.2	22
20	Aging behavior of Al-Li-(Cu, Mg) alloys processed by different deformation methods. Materials and Design, 2020, 196, 109139.	7.0	22
21	Effect of Copper Addition on Precipitation Behavior near Grain Boundary in Al–Zn–Mg Alloy. Materials Transactions, 2019, 60, 1688-1696.	1.2	20
22	Effects of texture and precipitates characteristics on anisotropic hardness evolution during artificial aging for an Al–Cu–Li alloy. Materials and Design, 2021, 212, 110216.	7.0	17
23	Origin of the influence of Cu or Ag micro-additions on the age hardening behavior of ultrafine-grained Al-Mg-Si alloys. Journal of Alloys and Compounds, 2017, 710, 199-204.	5.5	16
24	Critical Temperature in Bulk Ultrafine-Grained Superconductors of Nb, V, and Ta Processed by High-Pressure Torsion. Materials Transactions, 2019, 60, 1367-1376.	1.2	12
25	Microstructure evolution in a hydrogen charged and aged Al–Zn–Mg alloy. Materialia, 2018, 3, 50-56.	2.7	11
26	Enhancement of Strength and Ductility of Al-Ag Alloys Processed by High-Pressure Torsion and Aging. Metallurgical and Materials Transactions A: Physical Metallurgy and Materials Science, 2013, 44, 3221-3231.	2.2	10
27	Nanoscale characterization of FeNi alloys processed by high-pressure torsion using photoelectron emission microscope. Journal of Applied Physics, 2013, 114, .	2.5	10
28	Aging behavior and microstructure of aged excess Mg type Al^ ^#8211;Mg^ ^#8211;Si alloys after HPT processing. Keikinzoku/Journal of Japan Institute of Light Metals, 2013, 63, 406-412.	0.4	8
29	Early Stage Clustering Behavior in Al-Mg-Si Alloys Observed via Time Dependent Magnetization. Materials Transactions, 2016, 57, 627-630.	1.2	8
30	Effect of Copper Addition on the Cluster Formation Behavior of Al-Mg-Si, Al-Zn-Mg, and Al-Mg-Ge in the Natural Aging. Metallurgical and Materials Transactions A: Physical Metallurgy and Materials Science, 2018, 49, 5871-5877.	2.2	8
31	Effect of cooling rate on precipitation during homogenization cooling in excess Si type Al–Mg–Si alloy. Materials Letters, 2020, 278, 128363.	2.6	8
32	The possible transition mechanism for the meta-stable phase in the 7xxx aluminium. Materials Science and Technology, 2020, 36, 1621-1627.	1.6	8
33	Low-Temperature and High-Strain-Rate Superplasticity of Ultrafine-Grained A7075 Processed by High-Pressure Torsion. Materials Transactions, 2018, 59, 1341-1347.	1.2	7
34	Microstructures and the Mechanical Properties of the Al–Li–Cu Alloy Strengthened by the Combined Use of Accumulative Roll Bonding and Aging. Advanced Engineering Materials, 2020, 22, 1900561.	3.5	6
35	Aging Behavior of Ultrafine-Grained Al–Mg–Si–X (X = Cu, Ag, Pt, Pd) Alloys Produced by High-Pressure Torsion. Materials Transactions, 2014, 55, 640-645.	1.2	5
36	Muon Spin Relaxation Study of Solute–Vacancy Interactions During Natural Aging of Al-Mg-Si-Cu Alloys. Metallurgical and Materials Transactions A: Physical Metallurgy and Materials Science, 2019, 50, 3446-3451.	2.2	5

#	Article	IF	CITATIONS
37	Annealing Behavior of FeNi Alloy Processed by High-Pressure Torsion. Materials Science Forum, 0, 667-669, 313-318.	0.3	4
38	Effect of extrusion conditions on recrystallization texture in A6063 alloy. Keikinzoku/Journal of Japan Institute of Light Metals, 2019, 69, 327-331.	0.4	4
39	Effect of Cooling Rate on Precipitation during Homogenization Cooling in Balanced Al–Mg ₂ Si Alloy. Materials Transactions, 2020, 61, 2115-2120.	1.2	4
40	Aging behavior of ultrafine-grained Al^ ^ndash;Mg^ ^ndash;Si^ ^ndash;X (X=Cu, Ag, Pt, Pd) alloys produced by high-pressure torsion. Keikinzoku/Journal of Japan Institute of Light Metals, 2012, 62, 448-453.	0.4	3
41	Strengthening of Al 6061 Alloy by High-Pressure Torsion through Grain Refinement and Aging. Materials Science Forum, 2013, 765, 408-412.	0.3	3
42	Nanostructure control of age-hardenable Al 2024 alloy by high-pressure torsion. IOP Conference Series: Materials Science and Engineering, 2014, 63, 012083.	0.6	3
43	Precipitation structure and mechanical properties on peak-aged Al–Zn–Mg alloys including different with some Zn/Mg ratios. Keikinzoku/Journal of Japan Institute of Light Metals, 2017, 67, 162-167.	0.4	3
44	Effect of Thermal Cycles on Microstructure of Er ₂ O ₃ Thin Film on SUS316 Substrate with Y ₂ O ₃ Buffer Layer Fabricated by MOCVD Method. Materials Transactions, 2018, 59, 176-181.	1.2	3
45	Abnormally enhanced diamagnetism in Al-Zn-Mg alloys. Journal of Alloys and Compounds, 2019, 774, 405-409.	5.5	3
46	Corrosion Behavior of Crofer 22APU for Metallic Interconnects in Single and Dual Atmosphere Exposures at 1073~K. Acta Physica Polonica A, 2017, 131, 1394-1399.	0.5	3
47	Superplasticity of Ultra-Fine Grained 7075 Alloy Processed by High-Pressure Torsion. Materials Science Forum, 0, 794-796, 807-810.	0.3	2
48	The Effect of Thermal History on Microstructure of Er ₂ O ₃ Coating Layer Prepared by MOCVD Process. Plasma and Fusion Research, 2016, 11, 2405120-2405120.	0.7	2
49	Effect of copper on fine precipitates at the early stage of aging in Al–Mg–X (X=Si, Ge, Zn) alloys. Keikinzoku/Journal of Japan Institute of Light Metals, 2017, 67, 186-192.	0.4	2
50	Microstructure of Erbium Oxide Thin Film on SUS316 Substrate with Y ₂ O ₃ or CeO ₂ Buffer Layers Formed by MOCVD Method. Materials Transactions, 2017, 58, 231-235.	1.2	2
51	TEM Observation of Precipitates in Cast Al-7%Si-0.3%Mg Alloy Aged at 473 K. Journal of Smart Processing, 2019, 8, 155-159.	0.1	2
52	Aging Behavior of Al-Li-Cu-Mg Alloy Processed by High-Pressure Torsion. Materials Science Forum, 2010, 654-656, 1243-1246.	0.3	1
53	Dynamic Interactions between Precipitation and Plastic Deformation in Aluminium Alloys. Materials Science Forum, 0, 794-796, 1133-1140.	0.3	1
54	Three Strategies to Achieve Concurrent Strengthening by Ultrafine-grained and Precipitation Hardenings for Severely Deformed Age-hardenable Aluminum Alloys. Materia Japan, 2016, 55, 45-52.	0.1	1

⁵⁵ PM-21Microstructure observation of cold-rolled Al-Mg-Si alloy with Cu and Ag ad (Oxford, England), 2018, 67, i45-i45.	dition. Microscopy 1.	5 3	1
56 Formation of Erbia-Yttria double layer fabricated by metal organic chemical vapor with changing oxygen flow rates. Thin Solid Films, 2019, 689, 137455.	deposition process 1.	8 1	1
57 Texture formation process of 6063-type aluminium alloy during hot extrusion. M, Conferences, 2020, 326, 05005.	ATEC Web of o	.2]	1
58 Recent Research for Age-precipitation Sequence on Al-Mg-Si Alloys. Materia Japar	n, 2021, 60, 404-410. o	.1 1	1
59 Effect of Cu2+ Ion Irradiation on Microstructure of Er2O3 Coating Layer Formed Acta Physica Polonica A, 2017, 131, 1351-1353.	by MOCVD Method. o	.5 1	1
60 Effect of Sn and Rare Earth Elements on Mechanical Properties and Morphology 6 Graphite in FCD450 Cast Iron. Journal of Smart Processing, 2016, 5, 373-379.	of Spheroidal o	.1 1	1
61 Microstructure of Small Amount of TM Added Al-Mg-Si Alloys with Two-Step Agei Polonica A, 2017, 131, 1373-1376.	ng. Acta Physica o	.5]	1
62 TEM Observation of Cu and Ag Added Al-Mg-Si Alloy. Acta Physica Polonica A, 20	17, 131, 1379-1381. o	.5 1	1
63 Effect of Mn contents on Mg–6%Al alloys aged at 473 K. Keikinzoku/Journ Metals, 2018, 68, 480-486.	al of Japan Institute of Light o	.4]	1
 TEM Observation of HPT-Processed Cu-Added Excess Mg-Type Al-Mg-Si Alloys. Ma 0, 794-796, 811-814. 	aterials Science Forum, 0	.3 (0
65 Effect of HPT on Age-Hardening Behavior in Cu-Added Excess Mg-Type Al-Mg-Si A Materials Research, 0, 922, 487-490.	lloys. Advanced o	.3 (D
66 GRAIN REFINEMENT AND MICROSTRUCTURE EVOLUTION IN ALUMINUM A2618 TORSION. Jurnal Teknologi (Sciences and Engineering), 2016, 78, .	ALLOY BY HIGH-PRESSURE 0	.4 (0
67 Microstructure Observations of Graphite in Gray Cast Iron Using TEM. Materials S 879, 1911-1914.	Science Forum, 2016, 0	.3 (D
⁶⁸ The Effect of Sc Addition on Microstructure in Mg-Gd Alloys. Materials Science Fo 2239-2242.	orum, 2016, 879, 0	.3 (0
69 Fabrication and property evaluation of WO3 particles dispersed Al-based compos Web of Conferences, 2017, 130, 03002.	ite material. MATEC o	.2 (D
70 Effect of Addition of Inoculants and Solidification Structure on Machinability in F Iron. Journal of Smart Processing, 2017, 6, 81-86.	lake Graphite Cast 0	.1 (0
 Production of Al-based composite materials including stress-luminescent particle 3-dimensional penetration casting (3DPC). MATEC Web of Conferences, 2017, 1 	s using 30, 03003. 0	.2 (0

PM-16Influence of heat treatment on the structure of CrSiCN coatongs. Microscopy (Oxford,) Tj ETQq0 0 0 rgBT /Overlock 10 Tf 50 62 T

#	Article	IF	CITATIONS
73	PM-12Precipitates structure analysis of Mg-Y-Sc alloy by HRTEM. Microscopy (Oxford, England), 2018, 67, i41-i41.	1.5	0
74	PM-22Microstructure observation of HPT processed Al-2.5mass%Li(-2.0mass%Cu) alloy. Microscopy (Oxford, England), 2018, 67, i46-i46.	1.5	0
75	PM-11TEM observation of Al-1.0mass%Mg 2 Ge alloys with different elements. Microscopy (Oxford, England), 2018, 67, i40-i40.	1.5	0
76	PM-15Effect of Cu concentration on aiging behaviour and precipitation of Al-Zn-Mg Alloy with high Zn concentration. Microscopy (Oxford, England), 2018, 67, i42-i42.	1.5	0
77	PM-14Aging behavior of Al-7Si-0.4Mg casting alloy in T5 process. Microscopy (Oxford, England), 2018, 67, i42-i42.	1.5	0
78	PM-13Aging behavior of extruded Al-2.0%Mg-1.0%Si(mol%) alloy with and without homogenization. Microscopy (Oxford, England), 2018, 67, i41-i41.	1.5	0
79	PM-17Effect of cold-rolling on age hardenability of Al-1.0 mol%Cu-1.0 mol%Mg alloy. Microscopy (Oxford, England), 2018, 67, i43-i43.	1.5	0

80 PM-23 Microstructure observation of Ag added Al-Mg-Ge alloys aged at 523 K. Microscopy (Oxford,) Tj ETQq0 0 0 rgBT /Overlock 10 Tf 5

81	PM-10Fabrication and characterization of Mechanoluminescence particle dispersed Al based composite. Microscopy (Oxford, England), 2018, 67, i40-i40.	1.5	Ο
82	Muon Spin Relaxation of an Al–3.4%Zn–1.9%Mg alloy. , 2018, , .		0
83	Optimization of Mechanical Properties in Aluminum Alloys <i>via</i> Hydrogen Partitioning Control. Tetsu-To-Hagane/Journal of the Iron and Steel Institute of Japan, 2019, 105, 240-253.	0.4	Ο
84	Solute-vacancy clustering in Al–Mg–Si alloy studied by muon spin relaxation spectroscopy. Keikinzoku/Journal of Japan Institute of Light Metals, 2017, 67, 151-155.	0.4	0